FRET Analysis Indicates That the Two ATPase Active Sites of the P-Glycoprotein Multidrug Transporter Are Closely Associated[†]

Qin Qu and Frances J. Sharom*

Guelph-Waterloo Centre for Chemistry and Biochemistry, Department of Chemistry and Biochemistry, University of Guelph, Guelph, Ontario, Canada N1G 2W1

Received August 28, 2000; Revised Manuscript Received November 28, 2000

ABSTRACT: Members of the ABC superfamily carry out the transport of various molecules and ions across cellular membranes, powered by ATP hydrolysis. Substantial evidence indicates that the two catalytic sites of the nucleotide binding domains function in a highly cooperative, alternating sites mode, which suggests the possibility that they interact with each other physically. In this study, fluorescence energy transfer experiments were used to estimate the distance between two fluors, each covalently linked to a highly conserved Cys residue (Cys428 and Cys1071) within the Walker A motif of the catalytic site. The vanadate·ADP·Mg^{2+} complex was trapped in one catalytic site of membrane-bound or highly purified P-glycoprotein, and the other site was labeled with MIANS [2-(4′-maleimidylanilino)naphthalene-6-sulfonic acid]. Following loss of the trapped vanadate complex, the newly vacant site was then labeled with NBD-Cl (7-chloro-4-nitrobenzo-2-oxa-1,3-diazole). The fluorescence properties of the singly labeled P-glycoproteins showed that no energy transfer occurred between MIANS (the donor) and NBD (the acceptor) when they were simply mixed together. On the other hand, the fluorescence emission of the MIANS group in doubly labeled P-glycoprotein was highly quenched as a result of energy transfer to NBD, leading to an estimate of a donor−acceptor separation distance of ∼16 Å for P-glycoprotein labeled in the native plasma membrane and ∼22 Å for P-glycoprotein labeled in detergent solution. The separation of the two fluorophores is compatible with the recently reported crystal structure of the Rad50cd dimer, but not with that of the HisP dimer. These results suggest that the two catalytic sites of the P-glycoprotein nucleotide binding domains are relatively close together, which would facilitate cooperation between them during the catalytic cycle.

The ATP-binding cassette (ABC)[1] superfamily of membrane proteins comprises a group of diverse importers and exporters found in both prokaryotes and eukaryotes (*1*−*4*). ABC proteins are made up of a minimum of four modular units: two transmembrane (TM) domains, each typically with six membrane-spanning segments, and two nucleotide binding (NB) domains located on the cytosolic side of the membrane. The NB domains, which couple the energy of ATP hydrolysis to movement of substrates across the membrane, are highly conserved in this protein family (*5*). Each NB domain contains three characteristic sequence motifs: the Walker A and B motifs, which form the nucleotide binding site, and the so-called ABC signature sequence, or C motif, for which several functions have been proposed, including communication between the TM and NB domains during the transport cycle (*6*−*8*).

One member of the ABC superfamily, the P-glycoprotein multidrug transporter (Pgp), is implicated in the phenomenon of multidrug resistance in many human cancers (*9*). Pgp has been shown to transport a diverse range of nonpolar molecules, ranging from natural products such as the Vinca alkaloids to synthetic tripeptides. Physiologically, it plays an important role in preventing absorption of hydrophobic compounds in the gut (*10*), and makes a major contribution to the blood-brain barrier (*11*). The biochemistry and molecular pharmacology of Pgp have been extensively reviewed (*12*−*14*).

We currently have a rudimentary understanding of the way in which the two NB domains of Pgp operate during the catalytic cycle. Trapping of a vanadate transition state complex in the active site in one NB domain of Pgp completely eliminates catalytic turnover (*15*). These observations led to the proposal of an alternating sites mechanism (*16*−*18*), whereby only one active site can hydrolyze ATP at any point in time, and the two NB domains take turns. In other words, there is complete cooperativity between the two active sites. This proposal has been supported by covalent modification experiments and mutational analysis. If one of the two active sites is inactivated, either by reaction of *N*-ethylmaleimide with a Cys residue in the Walker A motif or by introducing a mutation into a highly conserved residue required for catalysis, all catalytic turnover stops (*19*, *20*). Covalent modification of Pgp with NBD-Cl also

[†] This work was supported by a grant to F.J.S. from the National Cancer Institute of Canada, with funds provided by the Canadian Cancer Society.

* To whom correspondence should be addressed: Department of Chemistry and Biochemistry, University of Guelph, Guelph, Ontario, Canada N1G 2W1. Telephone: (519) 824-4120, ext 2247. Fax: (519) 766-1499. E-mail: sharom@chembio.uoguelph.ca.

[1] Abbreviations: ABC, ATP-binding cassette; CHAPS, 3-[(3-cholamidopropyl)dimethylammonio]-1-propanesulfonate; DTE, dithioerythritol; FRET, Forster resonance energy transfer; MDR, multidrug resistance; MIANS, 2-(4′-maleimidylanilino)naphthalene-6-sulfonic acid; NB, nucleotide binding; Pgp, P-glycoprotein multidrug transporter; NBD-Cl, 7-chloro-4-nitrobenzo-2-oxa-1,3-diazole; TM, transmembrane.

10.1021/bi002035h CCC: $20.00
Published on Web 01/12/2001

demonstrated the compete cooperativity of the two NB domains (*21*).

How the observed functional cooperativity of the NB domains of Pgp may be related to the three-dimensional structure of the protein is not known. Cooperative interactions in soluble proteins often involve changes in the contacts between subunits of multimeric proteins, which suggests that the two NB domains of Pgp interact with each other physically. Currently, there is only very limited information available on the structural architecture of the NB domains of ABC proteins. A high-resolution crystal structure has been obtained for HisP, the NB subunit of the histidine permease (*22*). It shows a dimer of L-shaped subunits, each consisting of two segments: arm I, which contains the catalytic sites and the Walker A and B motifs, and arm II, which is proposed to be embedded in the membrane and contains the C motif. The two catalytic sites face away from each other in the crystal dimer. More recently, Jones and George have proposed a new model for the dimeric interaction between the two NB domains of ABC transporters (*4*). They argue that the SGG sequence within the C motif of one NB domain is directly involved in ATP binding and catalysis in the other NB domain, as seen in a different symmetry-related dimer of HisP. A structure similar to this was indeed recently reported for the catalytic domain of Rad50, a soluble protein that contains an ABC−ATPase fold (*23*). In the X-ray crystal structure of Rad50cd, the C motif of one protein promotes dimerization by binding to ATP in the partner molecule. In addition, on the basis of the results of studies where Cys residues in the two NB domains were cross-linked to each other, Loo and Clarke recently proposed that rather than facing outward, as in the HisP dimer crystal structure, the two NB domains face toward each other (*24*). All of these models are difficult to reconcile with the low-resolution electron microscopy structure of Pgp reported by Rosenberg et al. (*25*, *26*). These images show the NB domains projecting away from a central protein cylinder with a diameter of 80 Å, which presumably places the catalytic sites out of contact range. It is difficult to see how this would allow close cooperation between the two NB domains during the catalytic cycle.

In the absence of any high-resolution structural information, fluorescence spectroscopic studies have proved to be useful in dissecting the functional architecture of Pgp (for reviews, see refs *27* and *28*). For example, FRET studies allowed estimates of the distance of the catalytic sites in the NB domains of Pgp from the interfacial region of the bilayer, and suggested that they are either in close contact with the bilayer surface or embedded in the membrane (*29*). In this work, we use covalently linked fluors and Forster resonance energy transfer (FRET) to estimate the distance separating the conserved Cys residues in the Walker A motifs of the NB domains of Pgp. The results indicate that the two catalytic sites are relatively close together, as in the Rad50cd structure, which would facilitate their interaction during the transport cycle.

MATERIALS AND METHODS

Materials. 3-[(3-Cholamidopropyl)dimethylammonio]-1-propanesulfonate (CHAPS), disodium-ATP, 7-chloro-4-nitrobenzo-2-oxa-1,3-diazole (NBD-Cl), and sodium orthovanadate were purchased from Sigma Chemical Co. (St. Louis, MO). Asolectin was obtained from Fluka (Ronkonkoma, NY). MIANS was supplied by Molecular Probes (Eugene, OR).

Plasma Membrane Preparation and Pgp Purification. Plasma membrane vesicles were isolated from MDR CH^RB30 Chinese hamster ovary cells as described previously (*30*). Membrane vesicles were stored at −70 °C for no more than 3 months before being used. Highly purified Pgp was isolated from plasma membrane vesicles using CHAPS extraction, followed by lectin affinity chromatography on Con A-Sepharose, as described previously (*31*). The final product consisted of 90−95% pure Pgp in 2 mM CHAPS, 50 mM Tris-HCl, 0.15 M NaCl, and 5 mM $MgCl_2$ (pH 7.5). Purified Pgp was kept on ice and used within 24 h. The protein was quantitated by the method of Bradford (*32*) for the plasma membrane and by the method of Peterson (*33*) for purified Pgp, using bovine serum albumin (crystallized and lyophilized, Sigma) as a standard.

Measurement of Pgp ATPase Activity. Mg^{2+}-ATPase activity of membrane-bound and purified Pgp was determined by assessing the release of inorganic phosphate from ATP, as described previously (*34*, *35*), in the presence of 1 mM ATP and 5 mM Mg^{2+} at 37 °C.

Vanadate Trapping of Plasma Membrane-Bound Pgp and Purified Pgp. A stock solution of 100 mM sodium orthovanadate was prepared at pH 10, and an aliquot was boiled for 4 min before each use to degrade polymeric species. To quantitate inhibition of Pgp ATPase, various concentrations of vanadate were added to Pgp (∼2 μg of protein) immediately prior to starting the assay.

For reactivation of membrane-bound Pgp ATPase activity following vanadate trapping, 800 μg of the membrane protein was incubated for 20 min at 37 °C in Tris buffer [50 mM Tris-HCl, 0.15 M NaCl, and 5 mM $MgCl_2$ (pH 7.5)] in the presence of 1 mM ATP, 0.1 mM EDTA, and 200 μM vanadate, in a total volume of 1 mL. After incubation, the sample was washed twice with ice-cold Tris buffer at 4 °C, pelleting the sample at 100000*g* for 20 min. The pellet was resuspended in 1.5 mL of buffer and incubated at 37 °C, and at various times, aliquots were removed and the ATPase activity was determined.

To assess the reactivation of purified Pgp ATPase activity following vanadate trapping, 100 μg of protein was incubated for 20 min at 37 °C in 2 mM CHAPS/Tris buffer in the presence of 1 mM ATP and 200 μM vanadate, in a total volume of 1 mL. The mixture was then eluted through a Bio-Gel-P6 gel filtration column (Bio-Rad Laboratories, Mississauga, ON), which was pre-equilibrated with the same buffer. The eluate containing Pgp was incubated at 37 °C, and aliquots were removed at various times for ATPase activity determination.

Single and Double Labeling of Membrane-Bound Pgp with MIANS and NBD-Cl. To carry out labeling of a single NB domain of membrane-bound Pgp, ∼20 mg of protein was incubated at 37 °C for 20 min in Tris buffer in the presence of 1 mM ATP, 0.1 mM EDTA, and 200 μM vanadate, in a total volume of 10 mL. The reaction was stopped by the addition of 10 mL of ice-cold Tris buffer, and the membrane was washed twice by centrifugation at 100000*g* for 20 min. The pellet was resuspended at 4 mg/mL in Tris buffer, and divided into three aliquots. Purified Pgp was isolated from

one aliquot as described above, as a control. The other two aliquots were incubated separately with 30 μM MIANS at 22 °C for 30 min in the dark, in the presence of 200 μM vanadate. Unreacted MIANS was quenched with 1 mM DTE and removed by gel filtration on a column of Bio-Gel-P6 which had been pre-equilibrated with Tris buffer. The MIANS-labeled plasma membrane was then incubated at 37 °C for 3.5 h to allow the release of trapped ADP and vanadate, after which it was divided into two aliquots. From one aliquot, singly labeled MIANS−Pgp was purified as described above. The other aliquot was doubly labeled by incubation with 1 mM NBD-Cl for 2 h at 22 °C, followed by two washes with Tris buffer by centrifugation at 100000*g* for 30 min at 4 °C. Doubly labeled MIANS−NBD−Pgp was then purified from the labeled plasma membrane as described above. Control unlabeled Pgp, singly labeled MIANS−Pgp, and doubly labeled MIANS−NBD−Pgp were obtained from the same Pgp preparation. All protein concentrations were adjusted to ∼40 μg/mL, and asolectin (100 nm extruded vesicles; see ref *31*) was added to a final concentration of 0.5 mg/mL.

Rate of Reaction of MIANS and NBD-Cl with Native and Vanadate-Trapped Pgp. To determine the rate of reaction of MIANS and NBD-Cl with Cys residues in native and vanadate-trapped Pgp, purified protein was treated with 200 μM vanadate in the presence of 1 mM ATP in 2 mM CHAPS/Tris buffer at 37 °C for 20 min. Excess vanadate, ATP, and inorganic phosphate were removed by passing the sample through a Bio-Gel-P6 gel filtration column. Both vanadate-treated Pgp and an otherwise identical untreated Pgp preparation were adjusted to a protein concentration of ∼50 μg/mL. Labeling with MIANS was initiated by addition of 6 μL of a 2.5 mM MIANS solution to 500 μL of a Pgp solution to give a final concentration of 30 μM, and fluorescence was monitored continuously with excitation at 322 nm and emission at 420 nm. Labeling with NBD-Cl was initiated by addition of 5 μL of a 100 mM NBD-Cl stock solution to 500 μL of a Pgp solution to give a final concentration of 1 mM, and fluorescence was monitored continuously with excitation at 465 nm and emission at 523 nm. Since NBD-Cl also reacts with buffer and CHAPS, the NBD-Cl fluorescence was monitored continuously in 2 mM CHAPS/Tris buffer containing no Pgp, and the fluorescence traces of vanadate-treated and untreated Pgp were corrected accordingly.

Single and Double Labeling of Purified Pgp in CHAPS Solution with MIANS and NBD-Cl. To carry out labeling of a single NB domain of purified Pgp, ∼200 μg of purified protein was incubated in 2 mM CHAPS/Tris buffer at 37 °C for 20 min, in the presence of 1 mM ATP and 200 μM vanadate in a total volume of 1.5 mL. The sample was then passed through a Bio-Gel-P6 gel filtration column to remove excess ATP, vanadate, and inorganic phosphate. The eluate was divided into three aliquots; one was saved as control untreated Pgp, whereas the other two aliquots were incubated with 30 μM MIANS at 22 °C for 30 min in the dark in the presence of 200 μM vanadate. Unreacted MIANS was quenched with 1 mM DTE and removed by gel filtration on a Bio-Gel-P6 column pre-equilibrated with 2 mM CHAPS/Tris buffer. The labeled Pgp was incubated at 37 °C for 3.5 h to allow the release of trapped ADP and vanadate, and then divided into two aliquots. One was retained as singly labeled MIANS Pgp; the other aliquot was labeled with 1 mM NBD-Cl for 2 h at 22 °C and then passed through a Bio-Gel-P6 column pre-equilibrated with 2 mM CHAPS/Tris buffer, to give the doubly labeled product, MIANS−NBD−Pgp. All protein concentrations were adjusted to ∼40 μg/mL, and asolectin was added as described above.

The stoichiometry of NBD labeling of vanadate-trapped purified Pgp in CHAPS was determined as described previously for Pgp labeled within the membrane (*29*), except that the product was dialyzed exhaustively against water, and dissolved in 5% (w/v) SDS and 0.4 M NaOH over a period of 48 h before absorbance measurements were made.

Fluorescence Measurements. The quantum yield, Q_D, of singly labeled MIANS−Pgp in the presence of 0.5 mg/mL asolectin was determined at an excitation wavelength of 322 nm, relative to a standard solution of quinine sulfate in 0.1 N H_2SO_4, using polarizers oriented at the magic angle (54.7°) in both the excitation and emission beams. The quantum yield of singly labeled MIANS−Pgp was calculated using the equation

$$Q_{\mathrm{MIANS-Pgp}} = \left(\frac{F_{\mathrm{MIANS-Pgp}}}{F_{\mathrm{quinine}}}\right)\left(\frac{A_{\mathrm{quinine}}}{\mathrm{A}_{\mathrm{MIANS-Pgp}}}\right)Q_{\mathrm{quinine}} \quad (1)$$

where Q_{quinine}, the quantum yield of quinine, is known to be 0.5 in 0.1 N H_2SO_4, $F_{\mathrm{MIANS-Pgp}}$ and F_{quinine} are the integrals of the fluorescence of singly labeled MIANS−Pgp and quinine sulfate in the wavelength range of 350−600 nm, respectively, and $A_{\mathrm{MIANS-Pgp}}$ and A_{quinine} are the absorbances of singly labeled MIANS−Pgp and quinine sulfate at 322 nm, respectively. Scattering was corrected using unlabeled Pgp in the presence of asolectin at the same protein concentration. The quantum yield of singly labeled MIANS−Pgp was estimated to be 0.0791.

Fluorescence spectra were recorded on a PTI Alphascan-2 spectrofluorimeter (Photon Technology International, London, ON) with the cell holder thermostated at 22 °C. All spectra were measured with a 4 nm excitation and emission band-pass. Emission spectra of labeled Pgp were corrected using a built-in automatic correction system. The excitation wavelengths for the MIANS and NBD fluorophores were 322 and 465 nm, respectively, while emission was monitored at 420 and 523 nm, respectively, with 4 nm slits. Measured fluorescence intensities were corrected for light scattering using controls containing unlabeled Pgp. The inner filter effect was corrected at both the excitation and emission wavelengths as described previously (*31*, *36*, *37*) using the equation

$$F_{\mathrm{icor}} = (F_{\mathrm{i}} - B) \times 10^{0.5b(A_{\lambda\mathrm{ex}}+A_{\lambda\mathrm{em}})} \quad (2)$$

where F_{icor} is the corrected value of the fluorescence intensity, F_{i} is the experimentally measured fluorescence intensity, B is the background fluorescence intensity (caused mainly by lipid vesicle scattering), b is the path length of the optical cell in centimeters, and $A_{\lambda\mathrm{ex}}$ and $A_{\lambda\mathrm{em}}$ are the absorbances of the sample at the excitation and emission wavelengths, respectively.

Determination of the Parameters for FRET Analysis. The efficiency of resonance energy transfer (E) between the donor

Table 1: Spectral Parameters and Estimated Distances for Energy Transfer between MIANS Donor and NBD Acceptor Fluors in the Catalytic Sites of Pgp

system	overlap integral, J ($cm^3\ M^{-1}$)	efficiency of energy transfer, E (%)[a]	R_o (Å)	estimated distance, R (Å)[a]
plasma membrane	2.983×10^{-14}	96.4 ± 0.34	27.6	16.0 ± 0.26
purified	3.016×10^{-14}	78.0 ± 3.62	27.7	22.4 ± 0.78
purified + ATP	3.019×10^{-14}	74.1 ± 2.96	27.1	22.0 ± 0.38
purified + doxorubicin	3.051×10^{-14}	72.1 ± 1.49	24.4	21.0 ± 0.80
purified + ATP + doxorubicin	3.065×10^{-14}	73.0 ± 1.70	23.5	20.6 ± 0.87

[a] Separate determinations were carried out on three independent preparations for Pgp labeled while membrane-bound and Pgp labeled in a detergent solution. Means ± the standard error of the mean are indicated. ATP was added to a concentration of 3 mM and doxorubicin to a concentration of 40 μM, both of which are close to saturating (*31*). The refractive index was assumed to be 1.33, and the orientation factor κ^2 was taken to be $^2/_3$ (see Materials and Methods). The values of J and R_o are different in the presence of doxorubicin because of a very small shift in λ_{max}, and reduction in Q_D of the labeled Pgp on drug binding.

and acceptor can be written as

$$E = 1 - \left(\frac{F}{F_o}\right) \tag{3}$$

where F and F_o are the fluorescence intensities of the donor in the presence and absence of the acceptor, respectively. The efficiency of FRET is related to the inverse sixth power of the distance (R) between the donor and acceptor in an isolated donor−acceptor system:

$$R = R_o(E^{-1} - 1)^{1/6} \tag{4}$$

where R_o is the distance at which the efficiency of energy transfer is 50%. R_o can be calculated from

$$R_o = 9.8 \times 10^3 \times (J\kappa^2 Q_D n^{-4})^{1/6}\ \text{Å} \tag{5}$$

where J is the spectral overlap integral between the donor and acceptor in units of cubic centimeters per mole per liter (see Table 1). Q_D is the fluorescence quantum yield of the donor, and n is the refractive index of the medium between the chromophores, which was taken to be 1.33, that of a dilute aqueous solution (*40*). The orientation factor κ^2 was taken to be $^2/_3$. Small differences between the true and assumed values of κ^2 produce only small errors in calculated donor−acceptor distances (*38*). In addition, we determined the polarization values of singly labeled MIANS−Pgp and NBD−Pgp to be 0.33 and 0.43, respectively. Haas et al. (*39*) calculated the dependence of κ^2 on the orientation of the donor and acceptor when the transitions involved in energy transfer are of mixed polarizations. For two chromophores with polarizations of 0.3 and 0.4, they showed that the error in distances estimated by energy transfer using a κ^2 value of $^2/_3$ would be only approximately ±12%.

The spectral overlap integral (J) was determined using the integral equation

$$J = \frac{\int F_D(\lambda)\epsilon_A(\lambda)\lambda^4\,\delta\lambda}{\int F_D(\lambda)\,\delta\lambda} \tag{6}$$

where F_D is the fluorescence intensity per unit wavelength interval in the presence of donor only, ϵ_A is the molar extinction coefficient of the acceptor, and λ is the wavelength in centimeters. The fluorescence emission spectra of MIANS−Pgp were recorded using excitation at 322 nm, and the absorption spectra of NBD−Pgp were measured using a computer-interfaced Perkin-Elmer Lambda 6 UV−visible spectrophotometer (Perkin-Elmer, Norwalk, CT), with sample and references cells at 22 °C. J was calculated from the spectral data using a computer program designed solely for that purpose by U. Oehler (Department of Chemistry and Biochemistry, University of Guelph).

Analysis of the Distance between the Donor and Acceptor. The data for energy transfer between the MIANS and NBD fluorophores were analyzed using eq 4. Three independent determinations of R were carried out on three different preparations of Pgp labeled while in the membrane, and three different preparations of purified Pgp labeled in CHAPS solution.

RESULTS

Trapping of the Vanadate·ADP·Mg^{2+} Complex in Membrane-Bound and Purified Pgp. In this study, we have used Pgp in two different forms: the membrane-bound protein in its native state and highly purified Pgp in a detergent/lipid solution. The source of membrane-bound Pgp was plasma membrane vesicles from the highly drug-resistant cell line, CH^RB30, for which >80% of the ATPase activity, measured under the assay conditions (see Materials and Methods), can be attributed to Pgp (*31*). The Pgp in this vesicle preparation is able to transport various substrates, such as colchicine (*41*) and the tripeptide NAc-LLY-amide (*42*), at high rates. Highly purified, catalytically active Pgp was isolated from the CH^RB30 plasma membrane using differential detergent extraction with CHAPS, followed by lectin affinity chromatography (*31*).

Urbatsch et al. showed that if orthovanadate (V_i) is added to membrane-bound Pgp in the presence of ATP and a divalent cation (such as Mg^{2+}, Mn^{2+}, or Co^{2+}), one catalytic turnover takes place at a single NB domain, resulting in trapping of the transition state complex ADP·V_i·M^{2+} in the active site (*15*). Figure 1A shows that vanadate trapping results in (temporary) loss of the ATPase activity of Pgp in CH^RB30 vesicles; a 20 min incubation with 1 mM ATP, 5 mM Mg^{2+}, and 100 μM vanadate is sufficient to reduce the enzymatic activity to ~5% of the starting value. If excess ATP and vanadate are removed, and the trapped Pgp is subsequently incubated at 37 °C, there is slow loss of the transition state complex from the catalytic site, resulting in restoration of the ATPase activity over time (Figure 1B). Both membrane-bound and purified Pgp recovered their ATPase activity by a process that could be fitted to a single-exponential function, with $t_{1/2}$ values of 44 and 66 min, respectively, at 37 °C. This time frame is long enough to

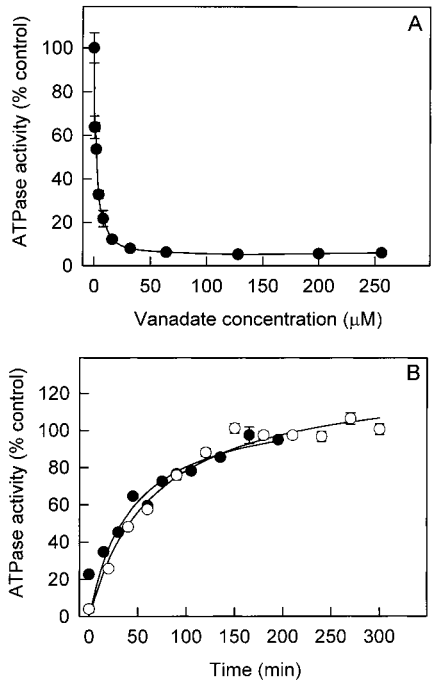

FIGURE 1: (A) Concentration dependence of inactivation of Pgp ATPase activity by orthovanadate in the presence of ATP and Mg^{2+} ions. The $CH^{R}B30$ plasma membrane (2 μg of protein) was incubated at 37 °C in the presence of 1 mM ATP, 5 mM Mg^{2+}, and increasing concentrations of vanadate. After 20 min, ATPase activity was measured as described in Materials and Methods. (B) Reactivation of Pgp ATPase activity at 37 °C following trapping of the $ADP{\cdot}V_i{\cdot}Mg^{2+}$ complex in the catalytic site of Pgp. The CH^{R}-B30 plasma membrane (~800 μg of protein) or highly purified Pgp (~100 μg of protein) was incubated with 1 mM ATP, 5 mM Mg^{2+}, and 200 μM vanadate for 20 min at 37 °C to produce the vanadate-trapped species. Following removal of vanadate as described in Materials and Methods, the Pgp sample was incubated at 37 °C for increasing times to allow release of the trapped $ADP{\cdot}V_i{\cdot}Mg^{2+}$ complex from the catalytic site, and ATPase activity was determined. Data are expressed as the percentage control relative to a sample of membrane-bound (●) or purified Pgp (○) that was treated identically, but in the absence of vanadate. The data were fitted to a single-exponential function, shown by the solid line; $t_{1/2}$ was estimated to be 44 and 66 min for membrane-bound and purified Pgp, respectively.

allow reactions to take place selectively at the other untrapped site (see below).

Single and Double Fluorescence Labeling of the Catalytic Sites in the NB Domains of Pgp. These trapping and release phenomena formed the basis of a strategy for single and double labeling at the NB domains of Pgp with different fluorophores, as shown in Figure 2. The $ADP{\cdot}V_i{\cdot}Mg^{2+}$ complex was trapped in one catalytic site of membrane-bound or highly purified P-glycoprotein, and the other unoccupied site was labeled with MIANS. Following loss of the trapped vanadate complex, the newly vacant site was then labeled with NBD-Cl. Vanadate dissociation is an efficient process, as indicated by the first work carried out by Urbatsch et al. on the trapping process (*15*), and the complete recovery of ATPase activity shown in Figure 1B. For Pgp that was labeled while in the plasma membrane, the purified protein in CHAPS was isolated from the membrane as described above. In the case of Pgp labeled in its purified form, the singly labeled and doubly labeled proteins were obtained directly in CHAPS solution.

Previous work in our laboratory indicated that MIANS and NBD-Cl react with Cys residues in both Walker A motifs of Pgp (*29*, *31*). When MIANS reacted with purified Pgp, it labeled two sites per molecule, as indicated by absorption spectroscopic measurements of the labeled protein product in 6 M guanidine hydrochloride (*31*). Labeling of membrane-bound Pgp with NBD-Cl also took place with a stoichiometry of two, also indicated by absorption spectroscopy (*29*). Labeling was carried out for both membrane-bound Pgp and purified Pgp for a technical reason. The second labeling step with NBD-Cl results in fluorescent side products in the case of purified Pgp, since the compound also reacts with the CHAPS necessary to maintain protein solubility. This complication is not present in the case of plasma membrane, which is handled in detergent-free buffer. In both cases, the final labeled purified Pgp product was studied in the presence of the phospholipid mixture asolectin (0.5 mg/mL), since membrane lipids appear to assist in maintaining the native state of the protein (*31*, *43*, *44*).

It should be noted that vanadate is trapped equally well in either NB domain (*15*), so this strategy produces Pgp labeled with MIANS in NB1 and NBD-Cl in NB2, and equal amounts of Pgp labeled with NBD-Cl in NB1 and MIANS in NB2. Since the two NB domains are perceived to operate in a completely symmetrical fashion, and no differences in their functioning during the catalytic cycle have yet been noted, both labeled forms are expected to behave identically. Pgp labeled at a single NB domain with either MIANS or NBD-Cl was produced by labeling the protein with a single fluorophore following vanadate trapping.

We first showed that vanadate trapping did in fact occlude one of the catalytic sites, making it unavailable for fluorescent labeling at the Cys residue. Purified Pgp was reacted with MIANS and NBD-Cl both in the absence of any treatment and following trapping of the $ADP{\cdot}V_i{\cdot}Mg^{2+}$ complex. MIANS and NBD-Cl become fluorescent only after covalent reaction with a −SH group, so the rate of increase of fluorescence intensity reflects the rate of reaction with Cys428 and Cys1071. Panels A and B of Figure 3 show that both reagents reacted with purified Pgp at approximately half the rate following vanadate trapping, consistent with the notion that one of the catalytic sites was unavailable. Thus, vanadate trapping blocks one of the active sites, allowing exclusive labeling of the other site. In addition, we determined the stoichiometry of single-site labeling in CHAPS of purified vanadate-trapped Pgp with NBD-Cl to be 1.1.

The fluorescence properties of the singly labeled Pgp species, for both MIANS and NBD-Cl, were compared to those of the doubly labeled proteins in which both sites are labeled with either MIANS or NBD-Cl in the absence of vanadate treatment. The fluorescence spectrum of Pgp labeled with MIANS at one NB domain (Figure 4A, curve b) was almost identical to that of the protein labeled at both NB domains (Figure 4A, curve a), with the exception that the emission intensity was reduced by approximately 50%. Similar results were obtained when comparing singly and doubly labeled NBD−Pgp products (data not shown).

FRET Analysis of Doubly Labeled Pgp. The emission spectrum of MIANS shows a large amount of overlap with the absorption spectrum of NBD-Cl, making this combination of fluors a good donor−acceptor pair for FRET studies (Figure 5A). We first ascertained whether NB domains in

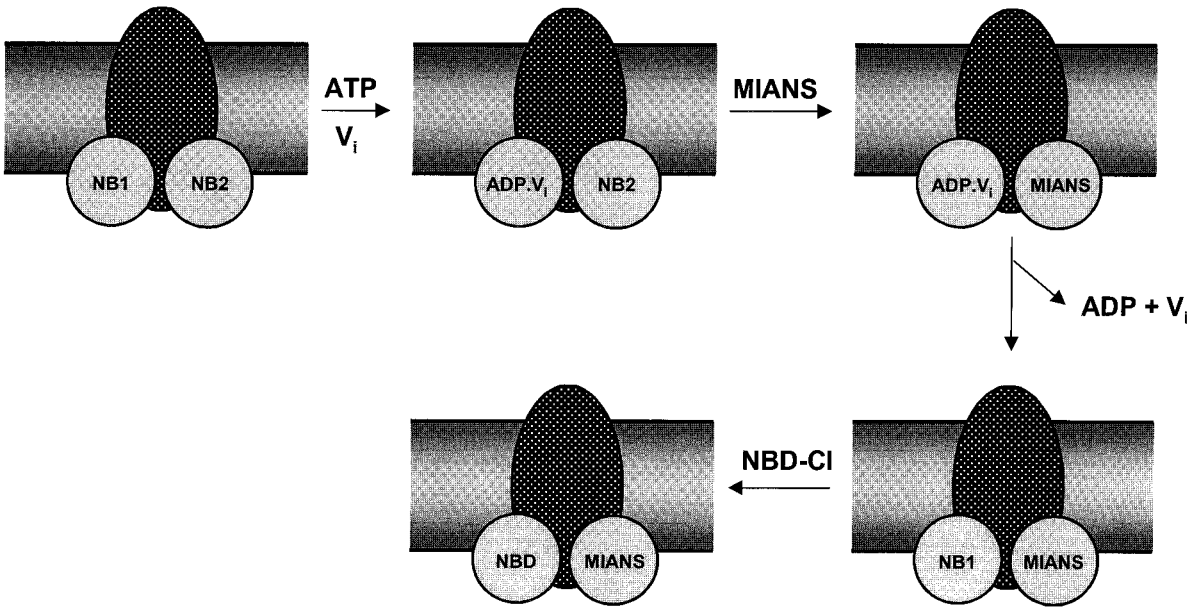

FIGURE 2: Schematic diagram of the strategy used to covalently link the donor fluor MIANS and the acceptor fluor NBD to Cys428 and Cys1071 in the catalytic sites of Pgp. Purified or membrane-bound Pgp was first incubated with 1 mM ATP, 5 mM Mg^{2+}, and 200 μM vanadate (V_i) at 37 °C for 20 min to trap the ADP·V_i·Mg^{2+} transition state complex at one of the catalytic sites (this is shown arbitrarily as NB1; both NB1 and NB1 will trap the complex equally well). Following removal of ATP and vanadate, the Cys residue of the empty NB domain was then reacted with MIANS. The transition state complex was allowed to leave the occupied NB domain by incubation at 37 °C for 3.5 h, and the newly vacated catalytic site was subsequently reacted with NBD-Cl.

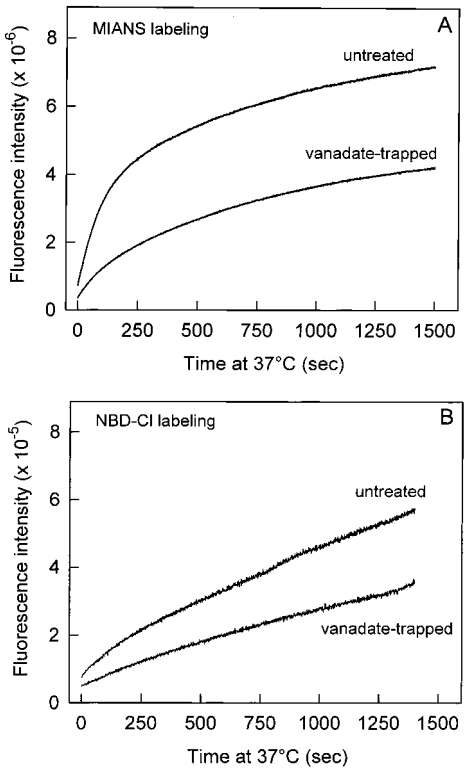

FIGURE 3: Time course of fluorescent labeling of purified Pgp in the native catalytically active state, and following trapping of the ADP·V_i·Mg^{2+} complex at one catalytic site. (A) Labeling by 30 μM MIANS at 22 °C, with a λ_{ex} of 322 nm and a λ_{em} of 420 nm. The protein concentration was 46 μg/mL in 2 mM CHAPS buffer. (B) Labeling by 1 mM NBD-Cl at 22 °C with a λ_{ex} of 465 nm and a λ_{em} of 523 nm. The protein concentration was 46 μg/mL in 2 mM CHAPS buffer. See Materials and Methods for details of the experimental labeling procedures.

neighboring Pgp molecules were able to transfer energy between each other. This situation might occur, for example, if dimer formation placed the NB domains of Pgp pairs close together. Radiation inactivation analysis suggested that Pgp exists as a dimer in the native plasma membrane (*45*), and detergent extracts were found to contain various oligomeric species (*46*). When singly labeled MIANS−Pgp was mixed in an equal mole ratio with unlabeled Pgp, the fluorescence intensity dropped by half (compare curves a and b of Figure 4B), as expected. After mixing of singly labeled MIANS−Pgp with singly labeled NBD−Pgp, there was a similar drop in intensity (Figure 4B, curve c). If FRET was taking place between the MIANS group in one Pgp molecule and the NBD in another neighboring molecule, then additional quenching of the MIANS fluorescence would have been expected as a result of energy transfer to the NBD moiety. Since this was not observed, we can assume that formation of Pgp dimers, if it takes place, does not contribute to FRET between adjacent protein molecules.

We then compared the fluorescence properties of doubly labeled MIANS−NBD−Pgp, where FRET might take place between the MIANS donor and the NBD acceptor, with those of the singly labeled MIANS−Pgp. For Pgp that had been labeled while in the native membrane-bound state and subsequently purified, there was a very large quenching of the MIANS fluorescence in the doubly labeled protein (Figure 5B), corresponding to an efficiency of energy transfer of >95% (Table 1). Sensitized emission from the NBD acceptor was visible, confirming that energy transfer was taking place. For Pgp that had been labeled in CHAPS solution, a lower degree of quenching was obtained, corresponding to an energy transfer efficiency of 78%. These measurements were highly reproducible for several independent preparations of both membrane-bound and purified Pgp. Using measured spectral parameters for the two fluors (Table 1), R_o for the donor and acceptor was calculated to be ~28 Å. Equation 4 (see Materials and Methods) was used to estimate the distance separating the two fluorophores. For

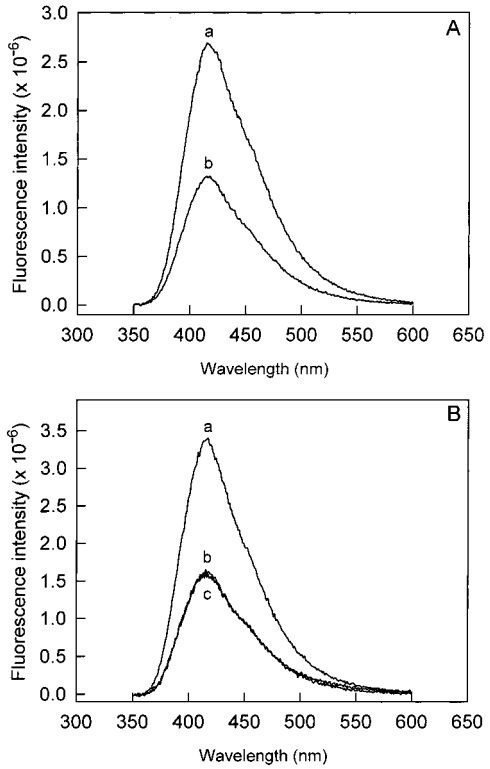

FIGURE 4: (A) Fluorescence emission spectra (λ_{ex} = 322 nm) of purified Pgp labeled at both NB domains with MIANS (curve a) and purified Pgp labeled at a single NB domain with MIANS following vanadate trapping (curve b). The same protein preparation was used for both labeling experiments, which were carried out in parallel. (B) Fluorescence emission spectra (λ_{ex} = 322 nm) of Pgp labeled at one NB domain with MIANS (curve a) and following 1:1 mixing with unlabeled Pgp (curve b) and following 1:1 mixing with Pgp labeled at a single NB domain with NBD-Cl (curve c). The protein concentration was 50 μg/mL in 2 mM CHAPS buffer with 0.5 mg/mL asolectin, and labeling was carried out for 30 min as described in Materials and Methods. Note that the experiments whose results are depicted in panels A and B were carried out on different Pgp preparations, so the fluorescence intensities cannot be compared between them.

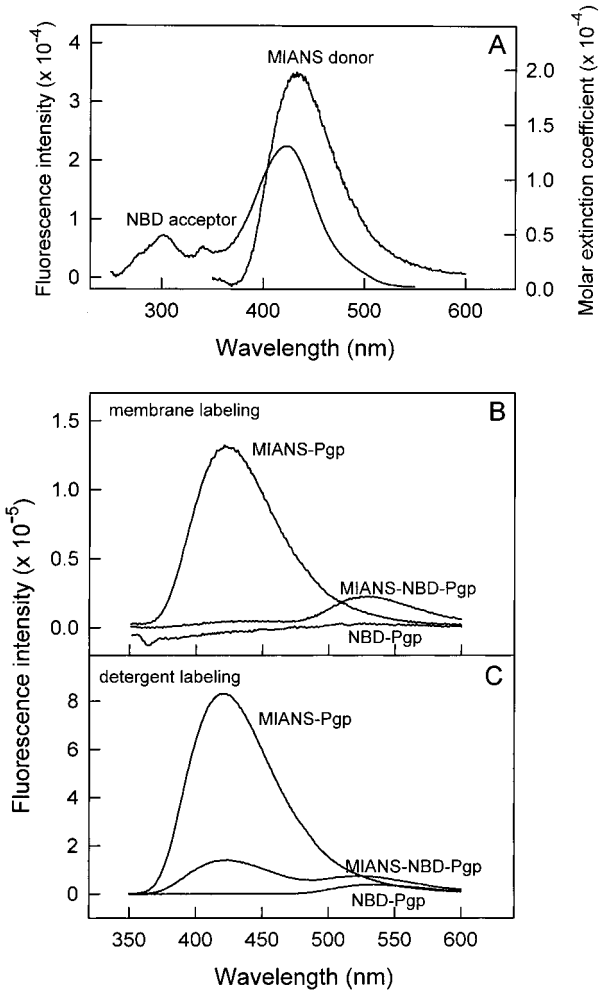

FIGURE 5: (A) Spectral overlap between MIANS−Pgp and NBD−Pgp. Fluorescence emission spectrum (λ_{ex} = 322 nm) of purified Pgp labeled at one NB domain with MIANS and the UV−visible absorption spectrum of purified Pgp labeled at one NB domain with NBD-Cl. (B) Fluorescence emission spectrum (λ_{ex} = 322 nm) of Pgp (40 μg/mL protein in 50 mM Tris-HCl buffer, 2 mM CHAPS, and 0.5 mg/mL asolectin) labeled while in the native membrane at a single NB domain with MIANS (MIANS−Pgp), compared to the fluorescence emission spectrum of the same preparation of Pgp singly labeled with NBD-Cl (NBD-Pgp), and doubly labeled with MIANS at one NB domain and NBD-Cl at the other (MIANS−NBD−Pgp). (C) Fluorescence emission spectrum obtained in an identical experiment, but carried out with purified Pgp labeled in a detergent solution, where the protein concentration was 40 μg/mL in 50 mM Tris-HCl buffer, 2 mM CHAPS, and 0.5 mg/mL asolectin.

Pgp labeled while membrane-bound, the donor−acceptor separation was estimated to be 16 Å, whereas Pgp labeled in CHAPS gave a slightly larger separation of 22 Å (Table 1). These results indicate that the two fluorescent groups, and by extension, the Cys residues within the Walker A motifs, are relatively close together.

The fluorophores used in these experiments have a finite size, so distance estimates represent the separation of the electronic centers of the two fluorophores. The maximum distance separating the two Cys residues to which the donor and acceptor are covalently linked can be estimated by accounting for the dimensions of the fluorophores (see below).

Doubly labeled MIANS−Pgp is still able to bind both nucleotides and drugs with unchanged affinity (*31*, *41*, *47*), and we have confirmed that this is also the case for doubly labeled NBD−Pgp (data not shown). To determine whether the separation distance between the two catalytic sites is altered by binding of ATP and transport substrates, the FRET measurements were also carried on purified Pgp in the presence of 3 mM ATP alone, 40 μM doxorubicin alone, and a combination of both. As indicated in Table 1, there was a small decrease in the distance between MIANS and NBD on binding of ATP alone, and doxorubicin alone. Binding of both ATP and drug resulted in a further decrease in the separation of the two fluorophores. The measured changes were relatively small, and indicate that substrate binding per se does not induce any gross changes in the placement of the two catalytic sites relative to each other.

Compatibility with Various Models of Pgp Structure. The high-resolution crystal X-ray dimer structures of the NB subunit of the histidine permease, HisP (*22*), and the catalytic domain of Rad50 (*23*), can be used to obtain information about the possible placement of the two NB domains of Pgp relative to each other. Both HisP and Rad50cd contain a Ser residue (Ser43 and Ser34, respectively) at the position equivalent to the Walker A Cys residues within Pgp that are labeled with MIANS and NBD-Cl. From the crystal coor-

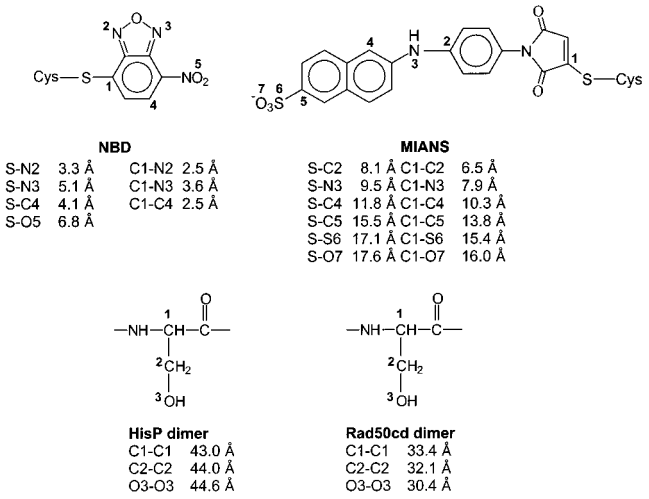

FIGURE 6: Molecular dimensions of the fluorophores were calculated by molecular mechanics using the program SPARTAN (Wavefunction, Inc.). Distances were estimated for the HisP and Rad50cd dimers from the crystal coordinate Protein Data Bank files using Rasmol.

dinates of the HisP dimer, we calculated the distance between the two Cα atoms of the Ser43 residue to be 43.0 Å. Distance estimates for the separation of other atomic pairs in the Ser side chain were slightly larger (see Figure 6), reflecting the placement of the two active sites facing away from each other. Similarly, we estimated the distance between the two Ser34 residues in the Rad50cd dimer that are equivalent to the labeled Walker A Cys residues. In this case, the distance between the two Cα atoms of Ser34 was calculated to be 33.4 Å. Separations of other atomic pairs in the Ser side chain are smaller (the O−O separation is 30.4 Å; see Figure 6), consistent with the two catalytic sites facing each other. The dimer model proposed by Jones and George (*4*) predicts a Ser O−O separation of 34 Å (A. M. George, personal communication), which is compatible with the Rad50cd dimer structure, but not with that of HisP.

To relate this information to the distance estimates obtained by FRET, the size of the donor and acceptor fluors must be taken into account. Molecular mechanics calculations were used to estimate the bond lengths and interatomic distances for the two fluorophores (see Figure 6 for selected distances). The NBD fluorophore is relatively small, with dimensions of ∼4−6 Å. The distance between the protein Cys S and the nitro group O is 6.8 Å. The MIANS molecule is considerably larger and elongated, with end-to-end dimensions from the protein Cys S to the sulfonate group of ∼17−18 Å. If the two S atoms of the Cys side chains are separated by ∼30 Å, as suggested by the Rad50cd dimer crystal structure and the model of Jones and George, and MIANS and NBD are arranged collinearly, the rough electronic centers of the fluorophores would appear to be ∼16 Å apart as assessed by FRET. The experimentally determined FRET separation for Pgp labeled in the membrane agrees well with this estimate. If the HisP dimer structure were in effect, the FRET separation would be expected to be substantially greater by ∼13 Å. Thus, our experimental data are compatible with the Rad50cd dimer structure and the Jones and George dimer model, but not with the HisP dimer structure. The orientation of the donor and acceptor fluorophores, and the Cys side chains, within the Pgp NB domains is unknown. If the fluorophores are collinear with the Cys residues, the distance between the two Cys residues in the NB domains estimated by FRET would be the maximum possible. Since the two active sites face each other in the Rad50cd and Jones and George models, this may in fact not be an unlikely scenario. If either fluorophore is rotated outward from a collinear arrangement, the Cys residues could approach each other more closely, while keeping the measured FRET separation at 16 Å. Thus, the FRET distance estimates indicate that the maximum separation of the two Walker A Cys residues is ∼30 Å, suggesting that the arrangement of the two NB domains in Pgp may be similar to that reported for the Rad50cd dimer, and the model of Jones and George.

DISCUSSION

The disposition of the NB domains of ABC transporters, with respect to both each other and the membrane, has been the object of much speculation. It has been proposed that these domains have a partial transmembrane orientation in the bacterial ABC permeases, where they are present as separate subunits. Possible projection of regions of the NB domains through the membrane would result in their accessibility to reagents at the extracellular (periplasmic) side. Proteolysis and biotinylation experiments indicated that this was indeed the case for the bacterial NB subunits, MalK in maltose permease (*48*) and HisP in histidine permease (*49*). Also, the X-ray structure of the HisP dimer suggested that arm II was embedded in the membrane (*22*). However, Higgins and co-workers used Cys insertions and reactivity with sulfhydryl-directed reagents to show that in the case of Pgp, the NB domains do not appear to be accessible at the external surface (*50*). Work in our laboratory has shown that the NB domains of Pgp are likely to be in contact with, or embedded in, the membrane bilayer (*29*), which would account for the ability of the host lipid to regulate the kinetic and catalytic properties of these domains (*51*).

In a recent study of cross-linking of Cys substitution mutants of Pgp, Loo and Clarke suggested that the orientation of the NB domains is such that the active sites face each other, in an organization quite different from that of the HisP dimer, where they have an outward-facing arrangement. Their results suggested that, since an introduced Cys at position 439 in NB1 and the endogenous Walker A motif Cys at position 1074 in NB2 could be readily cross-linked by disulfide bond formation, these residues may be located as close as 1 Å from each other. However, cross-linking only took place at 37 °C, not at the lower temperatures of 22 and 4 °C, which suggests that there may be considerable motion or flexibility in these regions of the protein. Cys cross-linking studies on the NB subunit of the maltose permease, MalK, also concluded that two residues predicted to lie in arm II, far apart from each other according to the HisP dimer structure, were actually located only 6−10 Å apart in dimeric MalK.

The modeling study of Jones and George (*4*) was the first to suggest that the C motif of one NB domain plays a central role in ATP binding in the catalytic site of the partner domain, in a reciprocal fashion. This proposal, which was supported by substantial biochemical and sequence evidence, helped to explain the requirement for two intact NB domains for catalysis, and their cooperativity, as well as the observation that protein function is highly sensitive to mutations in

the C motif. Thus there are good reasons to suspect that the arrangement seen in the HisP dimer structure may not reflect that of the two NB domains of Pgp. More recently, a high-resolution X-ray crystal structure of the catalytic domain of the soluble ABC protein Rad50 has been reported (*23*). It bears a remarkable resemblance to the HisP dimer model of Jones and George, and shows the two catalytic sites facing each other, with the C motif of one NB domain involved in binding the ATP γ-phosphate in the catalytic site of other NB domain.

In this study, we have made use of the vanadate trapping technique to selectively label a Cys residue within the Walker A motif of the two active sites of Pgp with the fluorophores MIANS and NBD-Cl. This double labeling procedure was performed on membrane-bound Pgp, followed by purification of the labeled protein, or alternatively, it was carried out directly on purified Pgp. Singly MIANS- and NBD-labeled proteins provided controls for characterization of the labeling process and the fluorescence studies. FRET experiments on the purified labeled Pgps in the presence of phospholipid indicated that there was highly efficient energy transfer between the MIANS and NBD molecules in doubly labeled Pgp. This translated into estimates of the separation distance of the two fluorophores of ~16 Å for Pgp labeled within a membrane environment, and ~22 Å for Pgp labeled in a detergent solution. After accounting for the size of the fluorophore molecules, these distance estimates are compatible with both the Rad50cd dimer structure and the Jones and George model, but not with the HisP dimer structure, which predicts a separation distance that is considerably larger, by ~13 Å. Our data also do not fit with the low-resolution structure of Pgp obtained by electron microscopy, which was interpreted as showing the NB domains projecting outward from a central toroidal structure 80 Å in diameter (*25*), presumably widely separated from each other.

The stoichiometry of MIANS labeling (two per protein and one per NB domain) was established previously (*31*), and for NBD-Cl labeling in a membrane environment, the number of labels was also determined previously to be two per protein (*29*). In addition, in this work, we showed that the stoichiometry of NBD labeling of purified vanadate-trapped Pgp in CHAPS is close to one. Since the stoichiometry of both MIANS and NBD labeling is well-established, the values of *R* derived from the FRET experiments have a low error associated with them, certainly small compared to the uncertainty of the orientation of the two fluorophores in the active site (see Figure 6). One possible reason for the difference in the estimated separation distance between Pgp labeled within the membrane and Pgp labeled in a detergent solution relates to our previous observation that Pgp ATPase activity in CHAPS solution is relatively uncoupled from drug binding, but coupling is restored when the protein is reconstituted into lipid bilayers (*52*). The presence of detergent may, therefore, "loosen up" the protein structure, which may result in an increased separation of the NB domains.

Our data showed a small decrease in the NB domain separation following binding of ATP and the transport substrate doxorubicin, and an additional decrease on binding of both molecules, suggesting that the two NB domains move closer together after substrate loading. However, these changes are small, suggesting that gross conformational rearrangements do not take place on binding of either nucleotide or drugs. These results are in agreement with our previous fluorescence quenching studies, which showed only small changes in the accessibility of the MIANS group (*47*) or Trp residues (*44*) to aqueous quenchers following binding of either ATP or drugs. It should be noted that the Ser34 separation distance calculated for the Rad50cd dimer is for the ATP-bound structure. Nucleotide is absolutely required for dimer formation; only monomers are present in the absence of ATP. Since it is not possible to obtain an estimate for the separation distance of these residues in the absence of ATP, the magnitude of the change in the relative placement of the two NB domains on nucleotide binding is not currently known. It seems likely that if a larger conformational change were to take place, it would be at the stage of the catalytic cycle where one of the NB domains is in the transition state. Unfortunately, we cannot use this type of species for the labeling approach employed in the study presented here, since vanadate trapping blocks labeling of the Cys residues with MIANS and NBD-Cl (Figures 3 and 4), and labeled Pgp is unable to progress through the catalytic cycle following substrate binding.

From previous work, it is known that the two NB domains of Pgp cooperate with each other in a tightly controlled fashion during the catalytic cycle. Vanadate traps the protein in a conformation in which one catalytic site is occupied with a transition state analogue and the other is inactive (*15*). It is widely believed that only one of the two active sites can function at any point in time, via an alternating sites type of mechanism (*17*). The ATP-induced dimerization behavior of Rad50cd, coupled with the dimer crystal structure, led to the suggestion that all ABC transporters operate by ATP-induced cycles of association and dissociation of the two NB domains (*23*). Since dissociation would probably require the hydrolysis of ATP to ADP at both catalytic sites, this may explain the tight coupling observed between the NB domains of Pgp. In any event, cooperative interactions of this type require that the two domains be physically close to each other.

REFERENCES

1. Doige, C. A., and Ames, G. F. (1993) *Annu. Rev. Microbiol. 47*, 291−319.
2. Holland, I. B., and Blight, M. A. (1999) *J. Mol. Biol. 293*, 381−399.
3. Van Veen, H. W., and Konings, W. N. (1998) *Adv. Exp. Med. Biol. 456*, 145−158.
4. Jones, P. M., and George, A. M. (1999) *FEMS Microbiol. Lett. 179*, 187−202.
5. Schneider, E., and Hunke, S. (1998) *FEMS Microbiol. Rev. 22*, 1−20.
6. Bakos, E., Klein, I., Welker, E., Szabo, K., Muller, M., Sarkadi, B., and Varadi, A. (1997) *Biochem. J. 323*, 777−783.
7. Hoof, T., Demmer, A., Hadam, M. R., Riordan, J. R., and Tummler, B. (1994) *J. Biol. Chem. 269*, 20575−20583.
8. Schmees, G., Stein, A., Hunke, S., Landmesser, H., and Schneider, E. (1999) *Eur. J. Biochem. 266*, 420−430.
9. Bosch, I., and Croop, J. (1996) *Biochim. Biophys. Acta 1288*, F37−F54.
10. Aungst, B. J. (1999) *Adv. Drug Delivery Rev. 39*, 105−116.
11. Schinkel, A. H. (1999) *Adv. Drug Delivery Rev. 36*, 179−194.
12. Sharom, F. J. (1997) *J. Membr. Biol. 160*, 161−175.

13. Ambudkar, S. V., Dey, S., Hrycyna, C. A., Ramachandra, M., Pastan, I., and Gottesman, M. M. (1999) *Annu. Rev. Pharmacol. Toxicol. 39*, 361−398.
14. Germann, U. A., and Chambers, T. C. (1998) *Cytotechnology 27*, 31−60.
15. Urbatsch, I. L., Sankaran, B., Weber, J., and Senior, A. E. (1995) *J. Biol. Chem. 270*, 19383−19390.
16. Senior, A. E., al-Shawi, M. K., and Urbatsch, I. L. (1995) *FEBS Lett. 377*, 285−289.
17. Senior, A. E., and Gadsby, D. C. (1997) *Semin. Cancer Biol. 8*, 143−150.
18. Senior, A. E. (1998) *Acta Physiol. Scand., Suppl. 643*, 213−218.
19. Loo, T. W., and Clarke, D. M. (1995) *J. Biol. Chem. 270*, 22957−22961.
20. Urbatsch, I. L., Beaudet, L., Carrier, I., and Gros, P. (1998) *Biochemistry 37*, 4592−4602.
21. Senior, A. E., and Bhagat, S. (1998) *Biochemistry 37*, 831−836.
22. Hung, L. W., Wang, I. X., Nikaido, K., Liu, P. Q., Ames, G. F., and Kim, S. H. (1998) *Nature 396*, 703−707.
23. Hopfner, K. P., Karcher, A., Shin, D. S., Craig, L., Arthur, L. M., Carney, J. P., and Tainer, J. A. (2000) *Cell 101*, 789−800.
24. Loo, T. W., and Clarke, D. M. (2000) *J. Biol. Chem. 275*, 19435−19438.
25. Rosenberg, M. F., Callaghan, R., Ford, R. C., and Higgins, C. F. (1997) *J. Biol. Chem. 272*, 10685−10694.
26. Higgins, C. F., Callaghan, R., Linton, K. J., Rosenberg, M. F., and Ford, R. C. (1997) *Semin. Cancer Biol. 8*, 135−142.
27. Sharom, F. J., Liu, R. H., and Romsicki, Y. (1998) *Biochem. Cell Biol. 76*, 695−708.
28. Sharom, F. J., Liu, R. H., Romsicki, Y., and Lu, P. H. (1999) *Biochim. Biophys. Acta 1461*, 327−345.
29. Liu, R., and Sharom, F. J. (1998) *Biochemistry 37*, 6503−6512.
30. Doige, C. A., and Sharom, F. J. (1991) *Protein Expression Purif. 2*, 256−265.
31. Liu, R., and Sharom, F. J. (1996) *Biochemistry 35*, 11865−11873.
32. Bradford, M. M. (1976) *Anal. Biochem. 72*, 248−254.
33. Peterson, G. L. (1977) *Anal. Biochem. 83*, 346−356.
34. Doige, C. A., Yu, X., and Sharom, F. J. (1992) *Biochim. Biophys. Acta 1109*, 149−160.
35. Sharom, F. J., Yu, X., Chu, J. W. K., and Doige, C. A. (1995) *Biochem. J. 308*, 381−390.
36. Lakowicz, J. R. (1999) in *Principles of Fluorescence Spectroscopy*, Kluwer Academic Publishers, New York.
37. Parker, C. A. (1968) in *Photoluminescence of Solutions*, Elsevier Publishing Co., Amsterdam.
38. Dale, R. E., Eisinger, J., and Blumberg, W. E. (1979) *Biophys. J. 26*, 161−193.
39. Haas, E., Katchalski-Katzir, E., and Steinberg, I. Z. (1978) *Biochemistry 17*, 5064−5070.
40. Wu, C. W., and Stryer, L. (1972) *Proc. Natl. Acad. Sci. U.S.A. 69*, 1104−1108.
41. Sharom, F. J., Lu, P., Liu, R., and Yu, X. (1998) *Biochem. J. 333*, 621−630.
42. Sharom, F. J., Yu, X., DiDiodato, G., and Chu, J. W. K. (1996) *Biochem. J. 320*, 421−428.
43. Doige, C. A., Yu, X., and Sharom, F. J. (1993) *Biochim. Biophys. Acta 1146*, 65−72.
44. Liu, R., Siemiarczuk, A., and Sharom, F. J. (2000) *Biochemistry* (in press).
45. Boscoboinik, D., Debanne, M. T., Stafford, A. R., Jung, C. Y., Gupta, R. S., and Epand, R. M. (1990) *Biochim. Biophys. Acta 1027*, 225−228.
46. Poruchynsky, M. S., and Ling, V. (1994) *Biochemistry 33*, 4163−4174.
47. Liu, R., and Sharom, F. J. (1997) *Biochemistry 36*, 2836−2843.
48. Schneider, E., Hunke, S., and Tebbe, S. (1995) *J. Bacteriol. 177*, 5364−5367.
49. Baichwal, V., Liu, D., and Ames, G. F. (1993) *Proc. Natl. Acad. Sci. U.S.A. 90*, 620−624.
50. Blott, E. J., Higgins, C. F., and Linton, K. J. (1999) *EMBO J. 18*, 6800−6808.
51. Romsicki, Y., and Sharom, F. J. (1998) *Eur. J. Biochem. 256*, 170−178.
52. Sharom, F. J., Yu, X., and Doige, C. A. (1993) *J. Biol. Chem. 268*, 24197−24202.

BI002035H